

**Supporting Information:**

**Development of thermodynamically-consistent  
machine-learning Equations of State: Application  
to the Mie fluid**

Gustavo Chaparro and Erich A. Müller\*

*Department of Chemical Engineering, Sargent Centre for Process Systems Engineering,  
Imperial College London, South Kensington Campus, London SW7 2AZ, U.K.*

E-mail: e.muller@imperial.ac.uk

The loss function, Eq. (S.1), used to train the FE-ANN EoS includes information from first-order derivative properties ( $Z$  and  $U^*$ ) and second-order derivative properties ( $C_V^*$ ,  $\gamma_V^*$ ,  $\rho^* \kappa_T^*$ ,  $\alpha_P^*$ ,  $\gamma$  and  $\mu_{JT}^*$ ). In the main article, the effect of different relative weights, Eq. (S.2), for the second-order derivative properties was discussed for  $w_i = 0, 1/20, 1/10$  and  $1$ . Other values of relative weights ( $1/50$  and  $1/5$ ) were also studied. The results of these models are found in Table S1.

$$\begin{aligned}\mathcal{L}^{prop} = & \frac{1}{N_p} \sum_{i=1}^{N_p} \omega_Z (Z_{i,MD} - Z_{i,model})^2 + \omega_{U^*} (U_{i,MD}^* - U_{i,model}^*)^2 \\ & + \omega_{C_V^*} (C_{V,i,MD}^* - C_{V,i,model}^*)^2 + \omega_{\gamma_V^*} (\gamma_{V,i,MD}^* - \gamma_{V,i,model}^*)^2 \\ & + \omega_{\rho^* \kappa_T^*} (\rho^* \kappa_{T,i,MD}^* - \rho^* \kappa_{T,i,model}^*)^2 + \omega_{\alpha_P^*} (\alpha_{P,i,MD}^* - \alpha_{P,i,model}^*)^2 \\ & + \omega_\gamma (\gamma_{i,MD} - \gamma_{i,model})^2 + \omega_{\mu_{JT}^*} (\mu_{JT,i,MD}^* - \mu_{JT,i,model}^*)^2\end{aligned}\quad (S.1)$$

with

$$\omega_i = \frac{w_i}{\sigma_i^2} \quad (S.2)$$

**Table S1: Trained FE-ANN EoS results<sup>a, b</sup>.**

Input Features	$w_i^c$	100×MSE								
		$Z$	$U^*$	$C_V^*$	$\gamma_V^*$	$\rho^* \kappa_T^*$	$\alpha_P^*$	$\gamma$	$\mu_{JT}^*$	
$\alpha_{vdw}, \rho^*, T^*$	0	Train	0.42	10.92	17.82	4.37	0.66	3.83	24.95	11.30
		Test	<b>0.32</b>	11.20	17.38	<b>3.12</b>	1.18	3.86	27.78	8.11
	1/50	Train	1.99	3.43	2.07	14.58	0.37	1.08	1.36	6.64
		Test	1.98	<b>3.27</b>	2.01	13.43	0.35	0.93	1.55	7.26
	1/20	Train	2.55	5.56	1.52	15.58	0.39	0.90	1.63	7.39
		Test	2.49	5.19	1.45	14.56	0.36	0.82	2.09	7.82
	1/10	Train	2.01	4.78	0.90	11.32	0.29	0.82	1.30	5.78
		Test	2.05	4.76	0.82	12.73	0.28	0.70	<b>1.48</b>	6.09
	1/5	Train	5.34	6.46	0.46	16.49	0.23	0.54	1.47	4.77
		Test	6.01	6.47	<b>0.46</b>	18.99	<b>0.26</b>	<b>0.64</b>	1.93	<b>4.56</b>
$\alpha_{vdw}, \rho^*, 1/T^*$	1	Train	31.44	29.53	0.65	60.45	0.51	0.68	3.01	5.05
		Test	34.63	31.74	0.72	71.85	0.53	0.95	3.63	4.67
	0	Train	0.21	2.16	11.94	2.33	0.92	2.47	26.58	11.73
		Test	0.16	1.97	11.54	1.40	3.10	2.90	28.11	10.99
	1/50	Train	1.99	7.44	2.85	5.57	0.49	1.37	1.62	7.24
		Test	2.52	8.02	2.77	6.73	0.48	1.29	1.78	7.52
	1/20	Train	0.18	0.55	0.35	0.79	0.15	0.62	0.89	5.50
		Test	<b>0.14</b>	<b>0.32</b>	0.33	<b>1.05</b>	0.15	0.57	<b>1.03</b>	5.72
	1/10	Train	0.26	0.83	0.32	0.83	0.11	0.49	0.88	4.61
		Test	0.26	0.64	<b>0.28</b>	1.37	<b>0.12</b>	<b>0.56</b>	1.21	<b>4.51</b>
	1/5	Train	0.43	1.30	0.27	1.20	0.10	0.43	1.09	4.44
		Test	0.42	1.03	0.25	2.13	0.13	0.65	1.73	4.07
	1	Train	7.87	9.02	0.37	7.22	0.27	0.55	2.15	4.82
		Test	8.03	8.57	0.34	10.26	0.29	0.76	2.72	4.20

<sup>a</sup> All the models consider a 4-layered neural network, activated using the tanh activation function and 45 neurons each. All models were trained for 20000 epoch using a learning rate of  $\alpha = 10^{-6}$  and the ADAM optimiser. <sup>b</sup> Smallest test MSE deviations are highlighted in **bold**. <sup>c</sup>  $w_i$  is the relative weight used for the second-order derivative properties in the loss function. This relative weight is set to 1 for the compressibility factor ( $Z$ ) and internal energy ( $U^*$ ). See Eq. (S.2) for further details.

# 1 FE-ANN EoS results for selected Mie Fluids

The main article presents the results of the FE-ANN EoS using  $\alpha_{vdw}$ ,  $\rho^*$  and  $1/T^*$  as input features and trained using a relative weight of  $w_i = 1/20$  for second-order properties for the Lennard-Jones fluid ( $\lambda_r = 12$  and  $\lambda_a = 6$ ). This section complements those results for other Mie fluids:  $\lambda_r = 16, 20, 24$  and  $30$  and  $\lambda_a = 6$ .

In Figures S1, S3, S5 and S7, the pressure isotherms for the mentioned Mie Fluids are shown. Similarly, in Figures S2, S4, S6 and S8, a list of second-order derivative properties are shown: (a) Isochoric Heat Capacity, (b) Isothermal Compressibility, (c) Thermal Expansion Coefficient, (d) Isobaric Heat Capacity, (e) Joule-Thomson Coefficient, (f) Thermal Pressure Coefficient.

For simplicity, all the figures shown below share the same nomenclature for symbols and lines. This is:

- Solid lines are FE-ANN EoS calculations
- Dashed lines are SAFT-VR-Mie EoS calculations
- Molecular dynamics data: (blue square)  $T^* = 0.9$ , (red square)  $T^* = 1.0$ , (black square)  $T^* = 1.3$ , (yellow square)  $T^* = 2.8$ , (purple square)  $T^* = 6.0$ .

## 1.1 $\lambda_r = 16$ and $\lambda_a = 6$

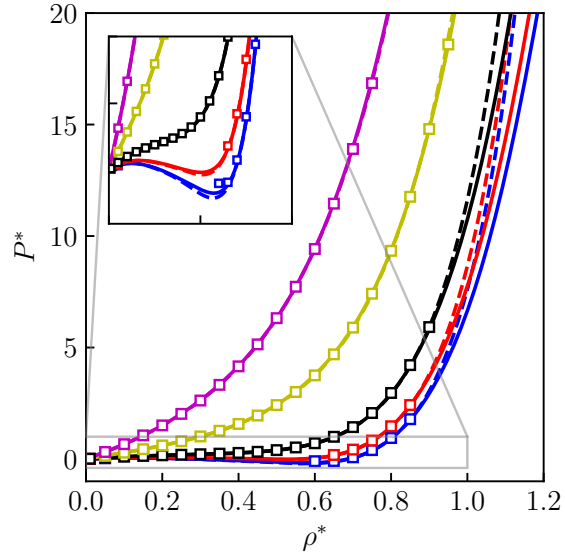


Figure S1: Pressure isotherms for the Mie fluid ( $\lambda_r = 16$  and  $\lambda_a = 6$ ).

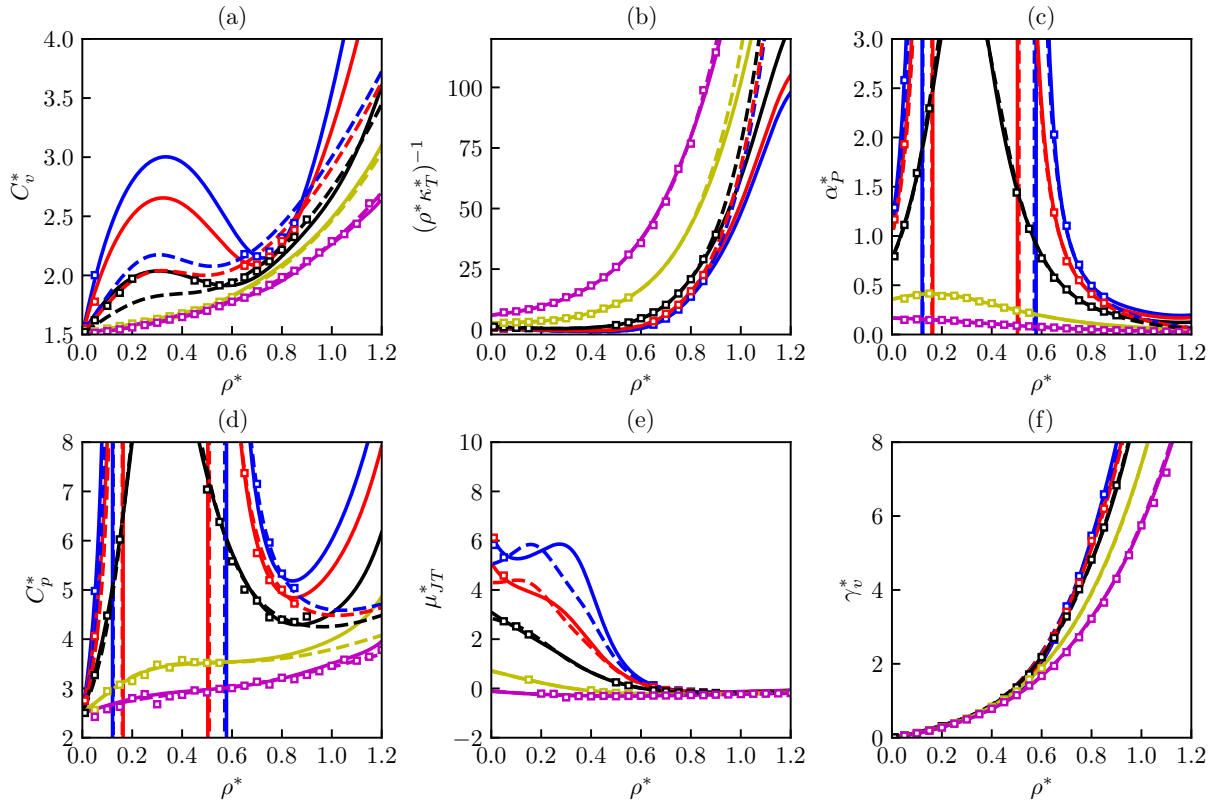


Figure S2: Second-order derivative properties isotherms for the Mie fluid ( $\lambda_r = 16$  and  $\lambda_a = 6$ ).

## 1.2 $\lambda_r = 20$ and $\lambda_a = 6$

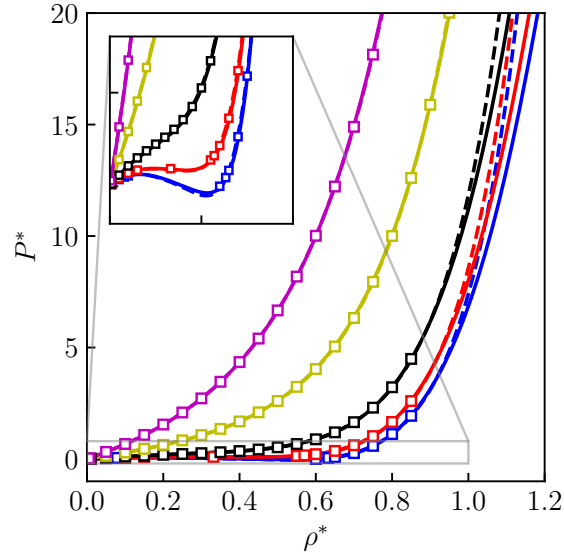


Figure S3: Pressure isotherms for the Mie fluid ( $\lambda_r = 20$  and  $\lambda_a = 6$ ).

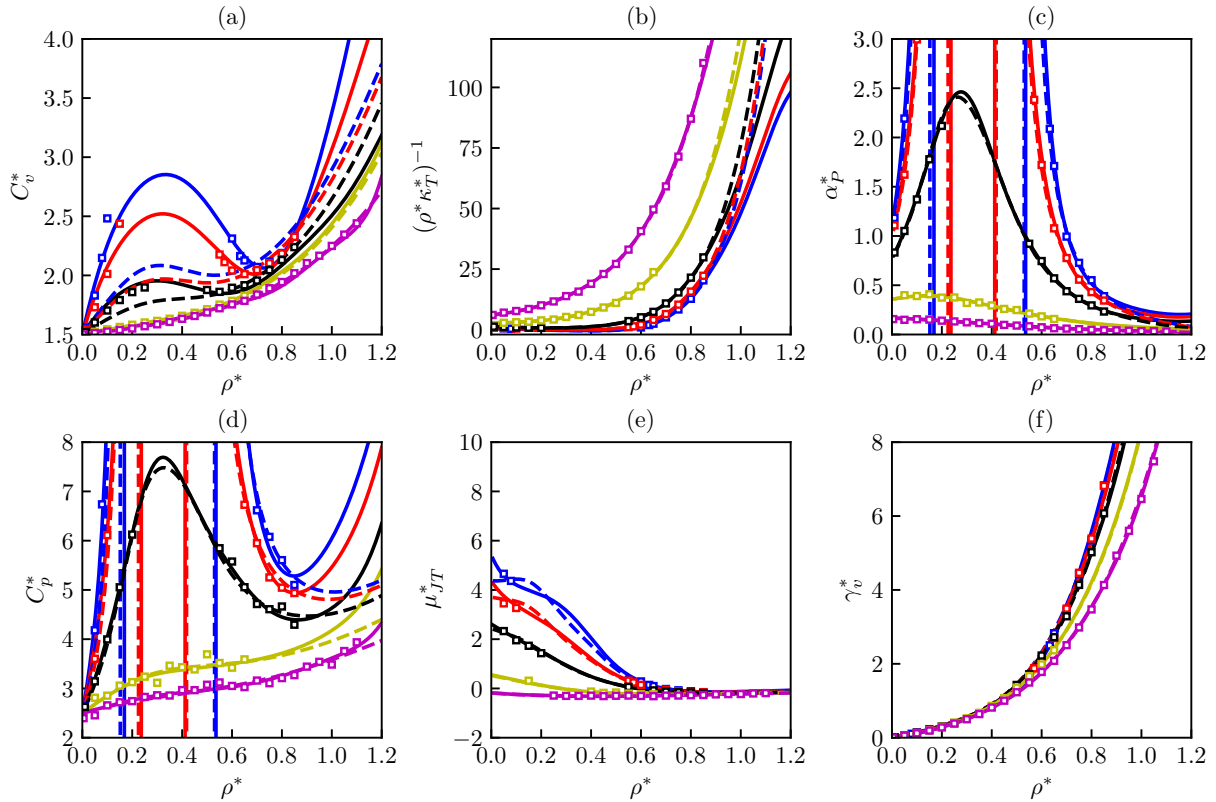


Figure S4: Second-order derivative properties isotherms for the Mie fluid ( $\lambda_r = 20$  and  $\lambda_a = 6$ ).

### 1.3 $\lambda_r = 24$ and $\lambda_a = 6$

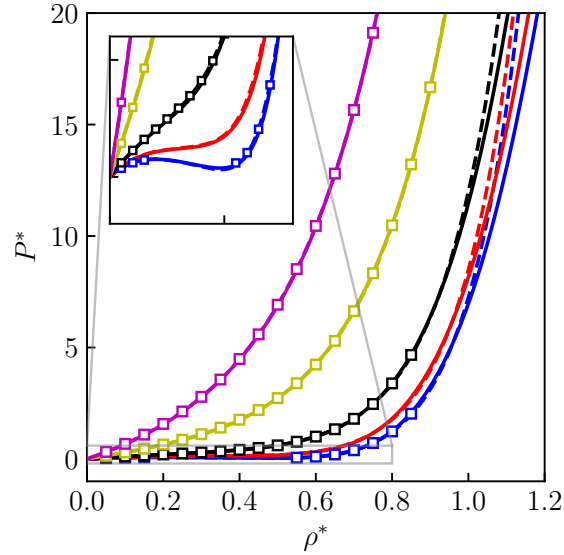


Figure S5: Pressure isotherms for the Mie fluid ( $\lambda_r = 24$  and  $\lambda_a = 6$ ).

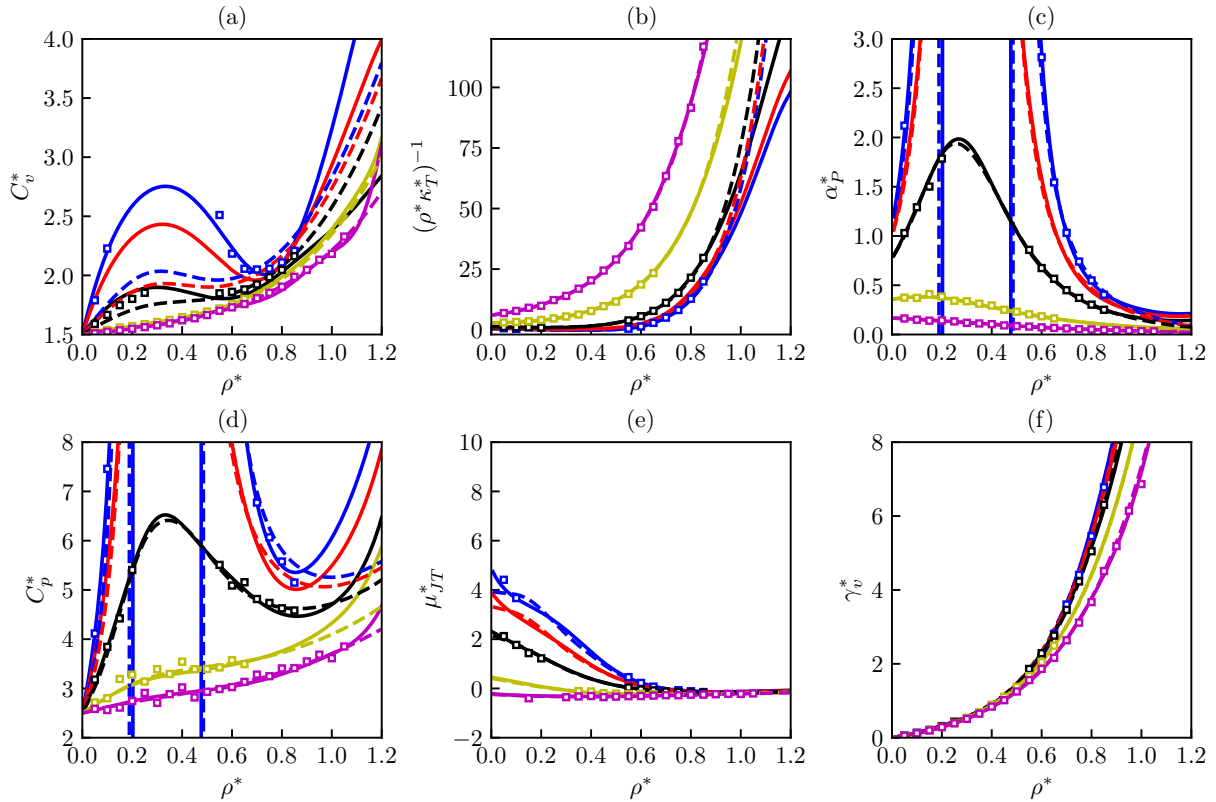


Figure S6: Second-order derivative properties isotherms for the Mie fluid ( $\lambda_r = 24$  and  $\lambda_a = 6$ ).

## 1.4 $\lambda_r = 30$ and $\lambda_a = 6$

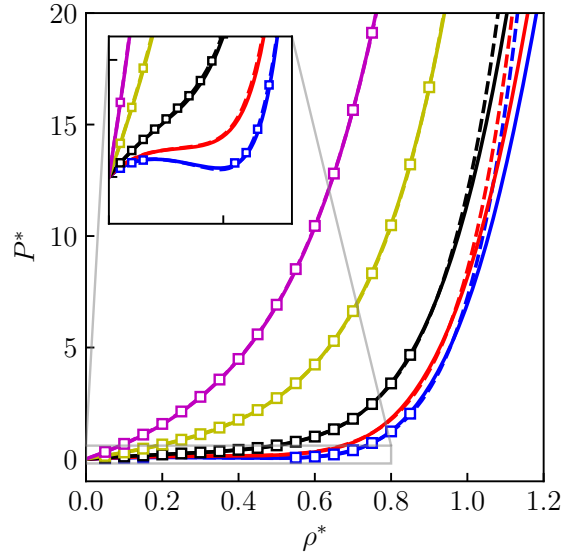


Figure S7: Pressure isotherms for the Mie fluid ( $\lambda_r = 30$  and  $\lambda_a = 6$ ).

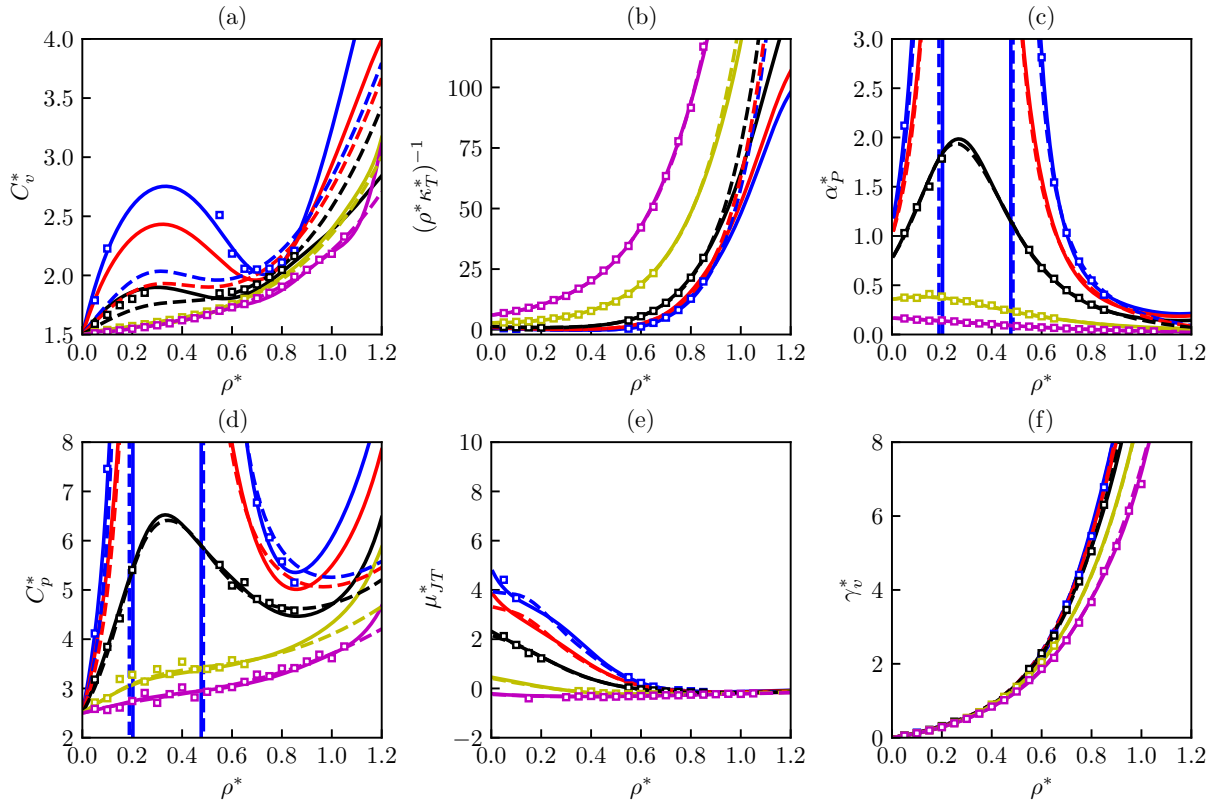


Figure S8: Second-order derivative properties isotherms for the Mie fluid ( $\lambda_r = 30$  and  $\lambda_a = 6$ ).